

Experimental characterization of non-premixed  
Hydrogen-Oxygen flames by LDV and Tomography measurements.

J.L. BEDUNEAU, A. BOUKHALFA and G. CABOT.

LAME CORIA UMR 6614 CNRS  
INSA Avenue de l'université-BP8  
76801 Saint Etienne du Rouvray Cedex.  
FRANCE

**Corresponding author:**

Prof. A. BOUKHALFA  
LAME CORIA UMR 6614 CNRS  
INSA Avenue de l'universite BP8  
76801 Saint Etienne du Rouvray Cedex France

PHONE:33.3.32.95.97.84

FAX:33.3.32.95.57.80

***E-mail: Mourad.Boukhalfa@coria.fr***

**Abstract:**

Velocity measurements and laser tomography visualization are performed for non-premixed flames stabilized on a coaxial injector. The aim of this study is to analyse the flame/turbulence interaction in the case of high speed flows. In this way, the study of hydrogen/oxygen flames characterized by an important heat release and a high Dämkoehler number, are of great interest since the flame/turbulence interaction are accentuated in comparison with other flames. Furthermore, the flow rates have been calculated to approach conditions similar to those of rocket engine with an important hydrogen excess and velocity ratio. Two optical diagnostic methods have been used to characterize the scalar and the dynamic structure of the flow field. Laser tomography is applied to visualize the flame location and two-components Laser Doppler Velocimetry (LDV) measurements is performed on flames to obtain velocity flow field.

The flow field structure of each flame was investigated by performing Laser Doppler Velocimetry (LDV) measurements. This flame produces a high temperature level ( 3000K ) and high flow velocity. The combination of this two conditions makes LDV measurements very complicate and increases the uncertainties of the experimental results. The flow seeding and the bias problems were simultaneously studied in this work. Laser tomography was also applied to visualize the flame location and to determine the global flame zone structure and the fresh gases inside the area within the conical flame

**1.Introduction:**

Coaxial jets are a simple and an efficient mixing way for two fluid streams. This geometrical concept has become a standard in recent years as an effective means to produce stabilized and well-controlled hydrogen-oxygen flames in rocket engine. However, the understanding of the interaction between the two flow fields of hydrogen and oxygen (i.e. their mixing and reacting areas) represents one of the major goal for the development of future high performance rocket engines.

In the present work, experiments are performed to investigate the flame dynamic and scalar structures under operating conditions obtained by hydraulic similarity with a real situation at atmospheric pressure and non-cryogenic condition.

These studies have investigated the effects of flow rate ratio ( $\frac{\rho U_{O_2}}{\rho U_{H_2}}$ ) and Reynolds number for two different exit diameters of coaxial injectors.

The flow field structure of each flame was investigated by performing Laser Doppler Velocimetry (LDV) measurements. This flame produces a high temperature level ( 3000K ) and high flow velocity. The combination of this two conditions makes LDV measurements very complicate and increases the uncertainties of the experimental results. The flow seeding and the bias problems were simultaneously studied in this work. Laser tomography was also applied to visualize the flame location and to determine the global flame zone structure and the fresh gases inside the area within the conical flame.

**2.Experimental set-up and flow field conditions:**

The type of injector used in this study presents a coaxial configuration (Fig 1), where oxygen is injected in the internal tube, with a mean exit velocity close to 10m/s and hydrogen in the outside one, with a mean exit velocity close to 60m/s. The combustion occurs at atmospheric pressure in an open square transparency combustion chamber of 60\*60 mm<sup>2</sup>. In this work, two geometrical configurations of coaxial injectors were studied. The main characteristics are represented in Table 1. In order to simulate the conditions in a rocket gas generator, injectors operate with an important excess of hydrogen. In such experimental conditions, the non-premixed hydrogen-oxygen flame is stabilized at the exit of the injector without any pilot flame, and the excess of hydrogen is burned with the air at the exit of the open combustion chamber.

This study was conducted using a parametrical approach, by varying the main dynamic and chemical parameters like injector diameter, flow rates and the mixing rate. (Table 2).

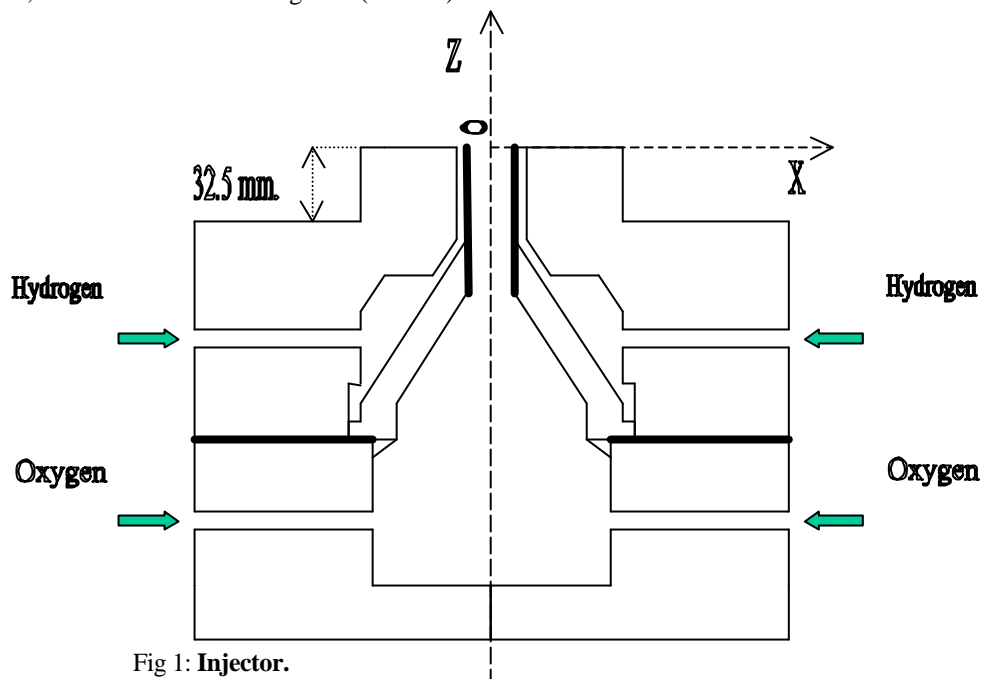


Fig 1: Injector.

	Diameter internal tube.	Diameter external tube.	Lip thickness.
<b>Injector 1.</b>	5.1mm.	9.1mm.	0.8 mm.
<b>Injector 2.</b>	6.6 mm.	11.7 mm.	0.8 mm.

Table 1: Geometrical characteristics of injectors.

		Hydrogen flow rate (g/s)	Hydrogen exit velocity (m/s)	Oxygen flow rate (g/s)	Oxygen exit velocity (m/s)	Oxygen Reynolds number	Flow rate ratio.	Mixing rate
<b>Injector 1.</b>	LF1	0,22	88	0,15	5,6	1780	0,7	0,98
	LF2	0,17	68	0,15	5,6	1780	0,9	0,76
	LF3	0,14	56	0,15	5,6	1780	1,1	0,62
	LF4	0,11	44	0,15	5,6	1780	1,3	0,49
<b>Injector2.</b>	LF5	0,38	82	0,256	2,8	2297	0,7	0,91
	LF6	0,29	63	0,256	2,8	2297	0,9	0,74
	LF7	0,24	52	0,256	2,8	2297	1,1	0,57
	LF8	0,19	41	0,256	2,8	2297	1,3	0,5

Table 2: Flow fields conditions.

For these conditions, the dynamic structure of each flame is investigated by performing LDV technique. This LDV system is a two colour, dual beam TSI system. Axial and radial velocity components are measured using respectively the green and the blue lines, from a 6 W Argon-Ion laser. Directional ambiguity for the radial component is eliminated by frequency shifting (40 Mhz on each beam pair). The LDV signal is processed by an IFA 750 Digital Burst Correlator. Both hydrogen and oxygen jets were seeded with Zirconium oxide ( $ZrO_2$ ) ( $diameter \approx 2 \mu m$ ) introduced in the flow by two rotative brush seeders. The LDV probe volume can be assumed to a cylindrical volume with 1.2mm length and 90  $\mu m$  diameter.

For all these conditions presented below, Laser Tomography is used to visualize the global structure of the flame. The tomographic system consists on a single Nd:YAG laser with second harmonic generating crystals used to create a Q-switched laser output at 532 nm. The laser sheet with a 200mJ/pulse energy illuminates the solid particles present in the flow. The flame images are recorded on CCD Kodak camera (Kodak Megaplus ES1) connected to a frame grabber Imasys, with a spatial resolution of 1008 x 1018 pixels<sup>2</sup>.

With such technique, the flame front is usually delimited by the interface separating the fresh gases (light region) and the products (black region). But in this case, with solid particles seeding and very hard conditions (expansion of the flow, high temperature and velocity gradient), this interface can not appears clearly. For these reasons, only qualitative results can be extracted from averaged images.

### 3. Velocity biases:

The LDV technique measure the instantaneous velocities of small seeding particles in the flow, which act as light scattering centres. The flow seeding is one of the most important aspects of LDV measurements particularly in these conditions. In fact these particles should be small enough to follow the local gas velocity, and resist to high temperature and high velocities conditions. Furthermore, the seeding homogeneity in all flames zones is a main problem for LDV measurements especially in the conditions of this study. In the present investigation, Zirconium oxide particles with 1-2  $\mu m$  diameter and fusion temperature estimated at 2900 K are used for seeding hydrogen and oxygen jets.

Three important biases have been examined [7] [10]: the effect of non-uniform seeding, the velocity gradient bias and the bias due to the refractive index gradients present at the boundaries of the burnt gas region.

In this region, where the temperature is very high, the incident laser beams can be defocused, deflected, or phase shifted, thus disturb the probe volume. According to Witze [10], it is shown that refractive index gradient caused by combustion has a negligible effect on both mean velocity and turbulence measurements, but can seriously debase the signal quality and thus the data rate. In our configuration, the data rate decreases in the oxygen potential core whether the seeding rate is higher. This is principally due to the crossing passage of the laser beams through the flame front. In these measurements, the seeding rate is adapted for this situation and velocity profiles seems to be correct and measured velocities correspond to those calculated with the theoretical flow rate.

The effect of non-uniform seeding is studied in the case of flame LF1. The results are presented in Figure 4 for three height locations in the flame.

For  $z=5$  and  $15\text{mm}$  sections (Fig 4 a,b), a high difference between velocity results with and without hydrogen flow seeding is observed. When the hydrogen jet is not seeded, the velocity is underestimated because at these sections the mixing phenomenon between hydrogen and oxygen is not important, so the hydrogen jet can not contain any solid particles. Therefore the velocity measured does not contain any information from the hydrogen flow. This phenomenon is enhanced by thermophoretics phenomena, especially at the injector exit where the flow regime is quasi-laminar.

At  $z=35\text{mm}$ , the mixing is more effective then the velocity profiles are quite similar.

In conclusion, for this study both flows have been seeded to avoid biases at the injector exit sections and near the flame zones.

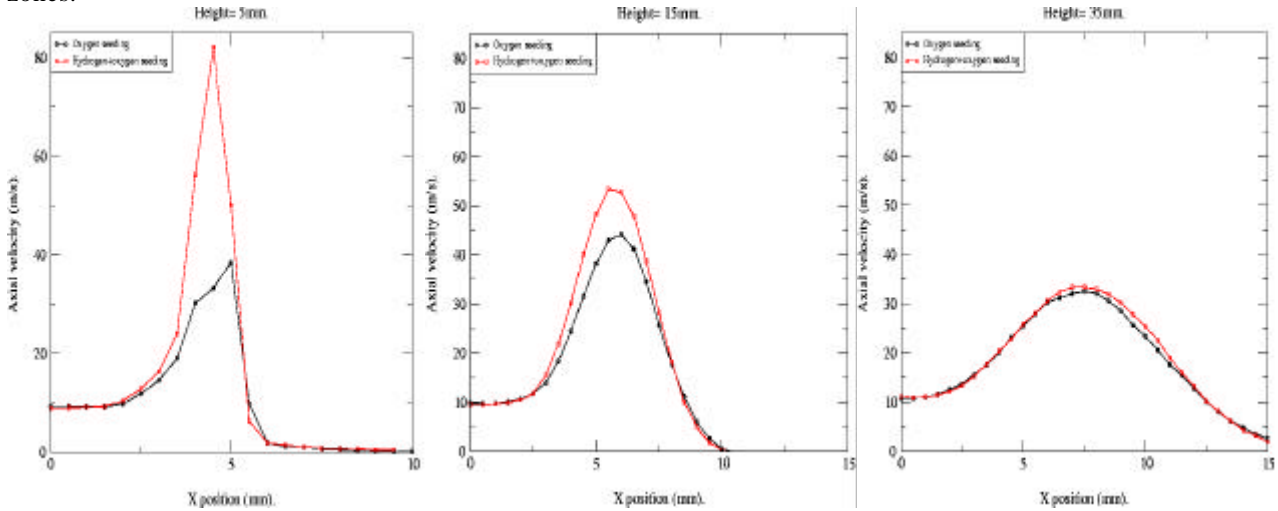


Fig 4 a,b,c: Axial velocities profiles for two seeding methods. (LF1)

Fig 5 presents an example of LDV measurements for both injectors obtained with the dual seeding. (hydrogen and oxygen flows):

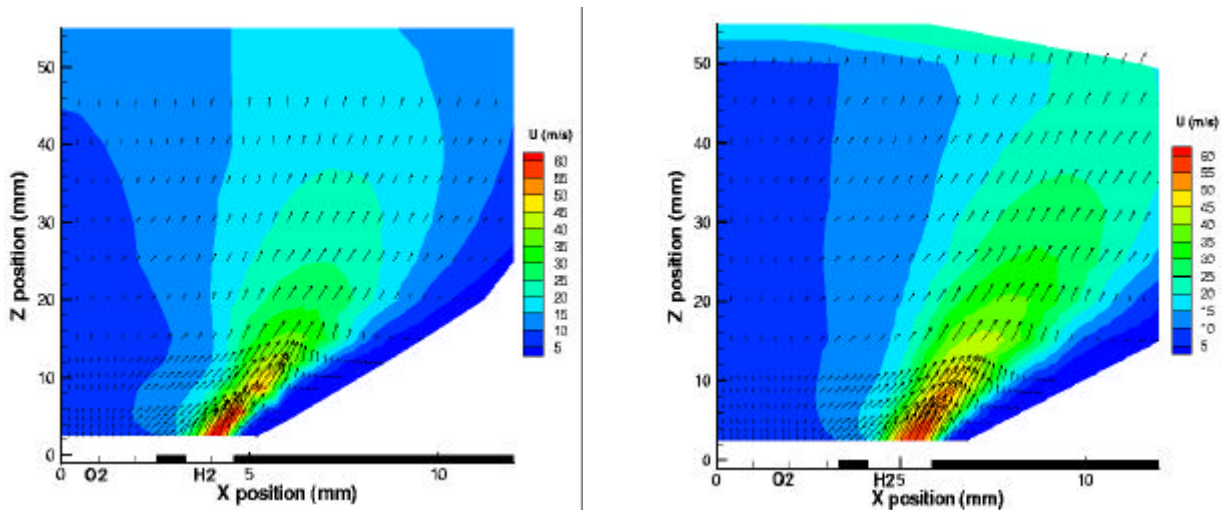


Fig 5 a,b: Velocity vectors for flames LF4 and LF8.

**4. Dynamic field structure:**

**4.a: Mean velocity evolution:**

Axial velocity profiles are reported in Fig.6,a and Fig.7,a for several axial positions. The same evolution is observed for both injectors. Three different zones can be observed:

The first zone corresponds to the oxygen potential core situated at the centre of the flame where the velocity values are globally constant. The second zone is represented by an important velocity increase with a very important gradient generated by the mixing area of hydrogen and oxygen, which corresponds to the combustion zone. And the third one is formed by the mixing zone of burnt gases and the hydrogen excess.

From these observations, we can consider the flow and the flame structure influenced by two majors phenomena which are the chemical reaction and the dynamic effects. These influences can be quantified by uncoupling these two

parameters.

**4.b: Normalized velocity evolutions:**

In this study, we consider that the maximum velocity observed for each profile characterizes the separation limit of each jet influences. Thus, a particular normalization of axial velocity can be proposed as suggested by [1,3,5].

Due to the two “mixing zones” situated within the flame zone and outside the flame it is necessary to apply an appropriate normalization for each mixing layer. With this particular normalization method, shear layers position are defined to be respectively  $x_{0,5int}$  and  $x_{0,5ext}$  for the internal and the external mixing layer.

The normalized mean velocity for the internal region is defined by:

1.For  $0 < x < x_{max}$  (internal region):

$$U_{norm}(x, z) = \frac{U(x, z) - U(0, z)}{U_{max} - U(0, z)} \text{ where } x=x_{0,5int} \text{ is obtained for } U_{0,5int} = \frac{1}{2}(U_{max} - U(0, z)) + U(0, z)$$

$U(0,z)$  is the velocity value at  $x=0$  and at  $z$  axial position.

2.For  $x > x_{max}$  (external region):

$$U_{norm}(x, z) = \frac{U(x, z)}{U_{max}} \text{ where } x=x_{0,5ext} \text{ is obtained for } U_{0,5ext} = \frac{1}{2} U_{max}$$

The results of this calculation are shown in figures 5b and 6b. This normalization takes into account only the dynamic parameters and not the chemical one’s.

A good agreement between these normalized profiles is globally observed for different axial positions. Indeed, this normalization reduces all the profiles as two inert mixing layers. The flame influence appears only at the beginning of the profiles increasing. It can be noted that for this location, a low discrepancy is observed for different normalized profiles, while a good similarity is obtained for the second mixing layer.

From these evolutions, we can conclude that the dynamic flame structure is governed by the dynamic exit conditions and not by chemical effects [6-7], excepted near the flame stabilization zone at the injector exit. In this region, the thermal effects are not negligible compared to the dynamic effects.

The flame region can be more precisely studied by using these normalisation results. Figures 6c and 7c show an enlargement view of the evolution of the normalized mean velocity versus the normalized radial location. At the injector exit ( $z=2.5mm$ ), the normalized profile gives smallest values. When  $z$  increases the normalized velocity increase until  $z=5mm$  for LF1 and  $z=10mm$  for LF5 and decreases for the other positions. At these positions, we suppose that the flame produces the maximum heat release in the flow and modify considerably the flow field.

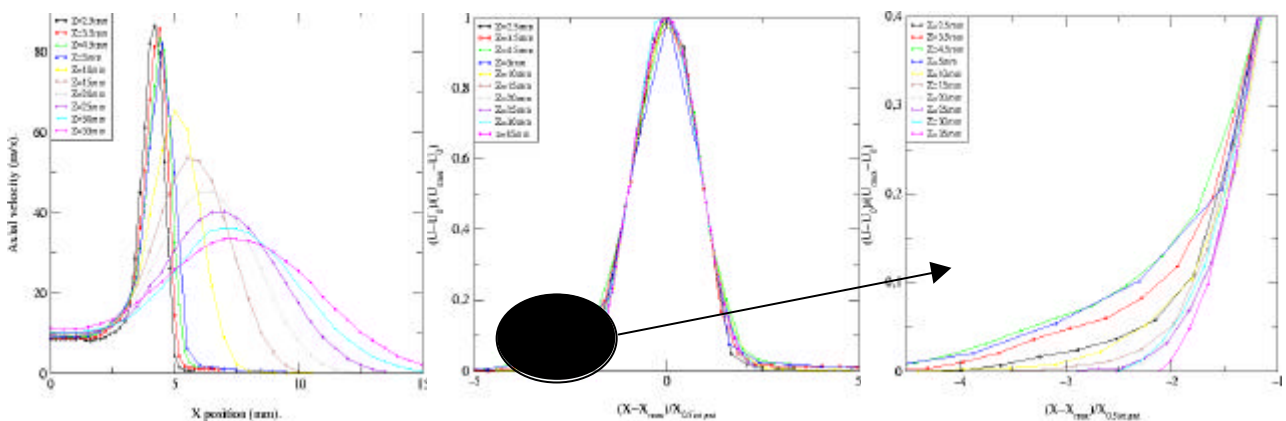


Fig 6.a: Axial velocity profiles (LF1)

Fig 6.b: Normalized axial velocity profiles (LF1).

Fig 6.c (LF1)

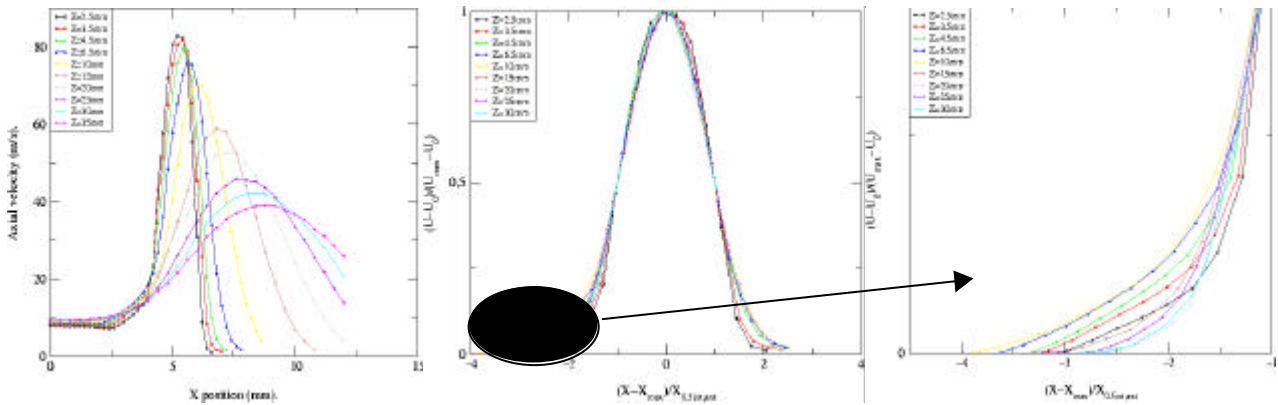


Fig 7.a: Axial velocity profiles (LF5) Fig 7.b: Normalized axial velocity profiles (LF5) Fig 7.c: (LF5)

In order to have a better understanding of the mean flow field structure of these flames, it is interesting to determine the location of the reaction zone and the external hydrogen jet influence. These parameters can be obtained by determining the position of the maximum velocity gradient in the flame zone ( $X_{0.5int}$ ) and in the external shear layer ( $X_{0.5ext}$ ), for each measured velocity profile. The evolution of these locations as a function of the axial position in the flame is presented in figure 8 for flames LF4 and LF8.

These figures show an important difference between the internal and the external flame region. The external mixing layer is composed of two zones. The first one situated at the injector exit is relatively short and evolves linearly with an important slope. The second one evolves quasi-linearly with a weaker slope. This evolution is quite similar to an inert mixing layer [3]. So, it can be concluded that the thermal effects are negligible on the external mixing layer.

The internal mixing and reacting zone evolution can be separated in two different linear zones. The first zone presents a linear evolution with a very important slope, and the second has also a linear evolution with a slope value varying from positive to negative when decreasing the diameters exit of injectors. This evolution results from the influence of the hydrogen jet on the flame region and prove that the dynamic structure of the hydrogen jet has a very great influence on the flame localisation.

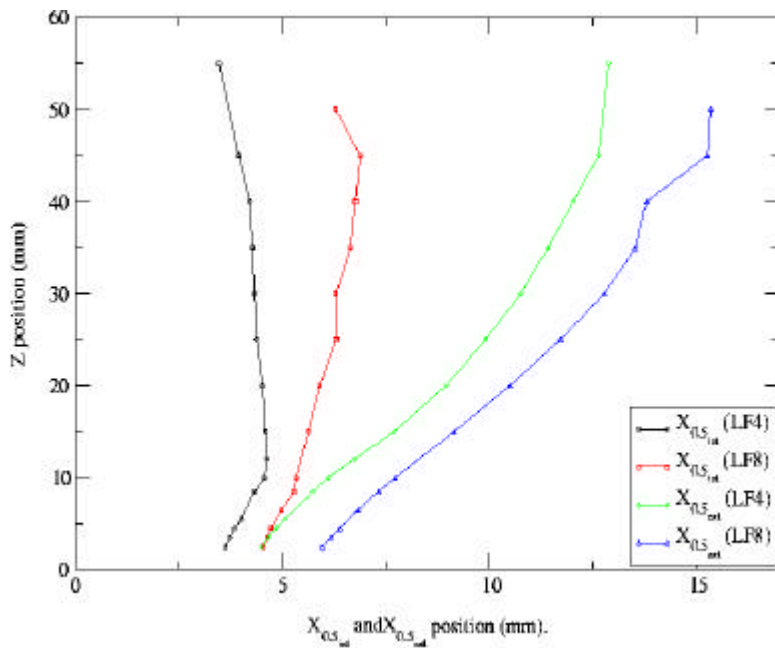


Fig 7:  $X_{0.5int}$  and  $X_{0.5ext}$  against Z position.

**5. Laser tomography:**

For all conditions studied below, the laser tomography technique is used to visualize the global flame structure, where Hydrogen and Oxygen flow are seeded by  $ZrO_2$  particles. Fig 9a shows an instantaneous tomographic recording. The oxygen potential core is clearly observed with a quite uniform particles repartition. The flame zone is clearly represented by the dark region where a little rate of particles are contained in the flow. The external bright region represent the excess Hydrogen jet and the mixing zone of burnt and unburned gases.

It is important to observed that the flame zone presents two different structures: the internal side corresponding to the oxygen interface is globally laminar and does not present any turbulence structures. However, the external interface of the flame zone (dark region) presents some large turbulence structures. Then, we can consider that the combustion regime is governed by the quasi-laminar oxygen jet in the internal side, but for the external side the combustion zone appears with large eddies which contribute to produce a high mixing flow.

A mean tomographic image (100 flames) is presented in fig 8a and 9b, for flames LF3 and F7. The three regions discussed below are clearly identified: the luminous potential core in the centre, the dark zone representing the flame location due to temperature increase (volumial expansion )and around it the luminous hydrogen flow.

From these images, some important parameters can be obtained. The flame height can be extracted by the determination of the internal flame front length. It can be noted that the flame LF3 (Fig 9b) obtained by a large injector diameter is longer than flame LF7 (Fig 8a). The flame zone thickness can also be obtained by calculating the dark region width on averaged images. The last parameter concerning the external mixing zone evolution can be determined by calculating the width of the external bright zone.

The results obtained by LDV and Tomography can be represented on the same figure in order to visualize simultaneously the scalar and the dynamic structure. We can observe that the location of the internal maximum gradient is located in the flame zone and the position of the external maximum gradient is situated nearly at the limit of the external bright zone which corresponds to the hydrogen excess and burnt gas mixing layer.

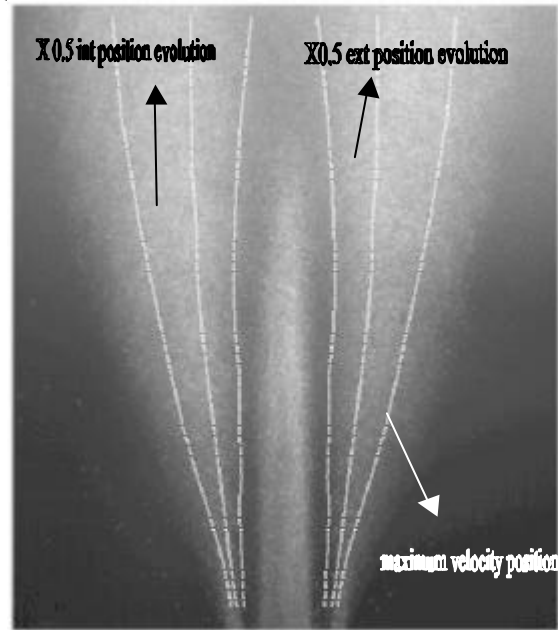


**Fig 8:** Averaged tomographic images obtained for 100 images (LF3).

**Fig8b:**Laser tomography image and LDV results

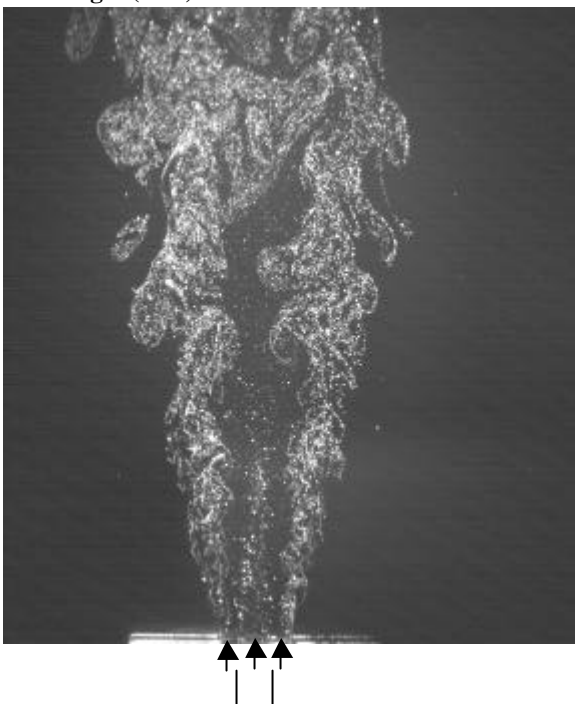


**Fig 9a: Instantaneous Tomographic image of H2/O2 Non-premixed flame, with ZrO<sub>2</sub> seeding (1mm=11pix)**

**Fig 9b: Averaged tomographic images obtained for 100 instantaneous images (LF7).**

### **6. Conclusion:**

The main objective of this investigation was to characterize the temperature zone action in a non-premixed hydrogen/oxygen flame and to determine the influence of each parameters on the flame flow field. In this way, a particular normalization type has been introduced.

A very good agreement has been obtained for each profiles for several conditions with this normalization which allows the thermal effects zone position to be defined. These effects are important at the injector exit near the flame stabilization position, with an action perceptible on laser tomographic images.

Internal and external shear layers evolution defined by  $x_{0.5int}$  and  $x_{0.5ext}$  position have been studied and show that thermal effects action on the internal shear layer seem to be mainly located between injector exit and  $2d_0$  ( $d_0$ =internal tube diameter). To progress in this phenomenon understanding, it is now necessary to have some information's on gas density ; this action is now in progress.

### **References:**

- [1] J.M BEER, N.A. CHIGIER (1964), "The flow region near the nozzle in double concentric jets". ASME 86D, J. Basic Eng., Vol.4, pp. 797-804.
- [2] N.T. CLEMENS (1995), "Effects of heat release on the near field flow structure of hydrogen jet diffusion flames", Comb. Flame, Vol. 102, pp. 271-284.
- [3] P. CHAISSAING (1979), "Melange turbulent de gaz inert dans un jet tube libre." These d'état Toulouse, Université Paul Sabatier, Toulouse.
- [4] H. REHAB et al. (1997), "Flow regimes of large-velocity-ratio coaxial jets". J. Fluid Mech. , Vol. 345, pp. 357-381.
- [5] J.C SACADURA (1997), "Etude expérimentale des flames non-premelangees hydrogene-oxygene. Caractérisation des champs dynamiques et scalaires." These de doctorat de l universite de Rouen.
- [6] J.C. SAUTET, D. STEPOWSKI (1995), " Dynamic behaviour of variable-density, turbulent jets in their near development fields", Phys. Fluids, Vol. 7, N. 11, pp. 2796-2806.
- [7] J.C. SAUTET (1992), "Effets des differences de densites sur le developpement scalaire et dynamique des jets turbulents." Thèse de doctorat de l'universite de Rouen.
- [8] J.P. SISLAIN et al. (1988), " Laser Doppler Velocimetry investigation of the turbulence structure of axisymmetric diffusion flames". Prog. Energy. Comb. Science, Vol. 14, pp. 99-146.
- [9] T. TAKAGI et al. (1981), " Properties of turbulence in turbulent diffusion flames." Combust. Flame, Vol. 40, pp. 121-140.
- [10] P.O. Witze, T.A. Baritaud (1985), "Influence of combustion on laser Doppler velocimeter signal quality in a spark ignition engine", ASME, 33.